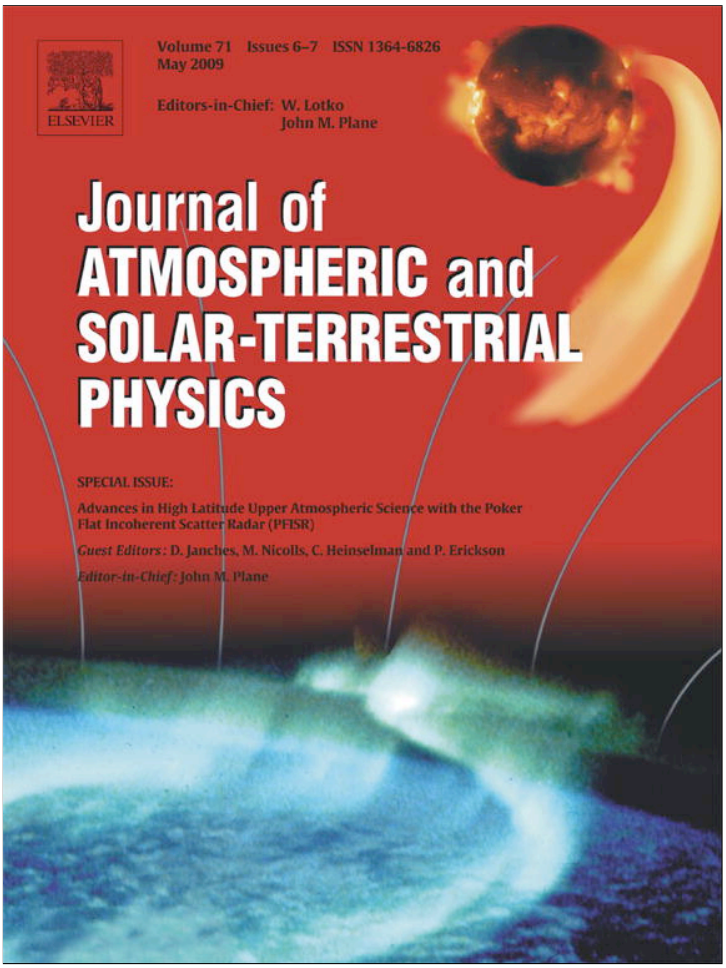

Journal of Atmospheric and Solar-Terrestrial Physics 71 (2009) 688–696

Contents lists available at ScienceDirect

Journal of
Atmospheric and Solar-Terrestrial Physics

journal homepage: www.elsevier.com/locate/jastp

Observations of D-region structure and atmospheric tides with PFISR during active aurora

D. Janches [a,*], D.C. Fritts [a], M.J. Nicolls [b], C.J. Heinselman [b]

[a] NorthWest Research Associates Inc., CoRA Division, 3380 Mitchell Lane, Boulder, CO 80301, USA
[b] Center for Geospace Studies, SRI International, 333 Ravenswood Avenue, Menlo Park, CA, USA

ARTICLE INFO

Article history:
Accepted 21 August 2008
Available online 18 September 2008

Keywords:
D-region
MLT
Tides

ABSTRACT

We report on combined spectral measurements of the D-region ionosphere and the polar summer mesosphere and lower thermosphere performed on 9 June 2007 with the 450 MHz Poker Flat Incoherent Scatter Radar (PFISR) under active auroral conditions. Observations during the first 7 h occurred at nighttime and revealed strong temporal correlations between enhanced auroral precipitation, the occurrence of polar mesosphere summer echoes (PMSE), and enhanced electron densities (N_e) extending to much lower altitudes (~60–80 km) than the previously reported at these latitudes without the presence of a polar cap absorption (PCA) event. PMSE and lower D-region echoes most often occurred together and PMSE were more often visible to PFISR before the N_e of the D-region was sufficiently high to be detected. These measurements also enabled definition of high precision horizontal winds (errors of 2–3 m s^{-1}) in the ~64–90 km altitude range, which has previously been possible only with MF and HF radars, with the Arecibo 430 MHz IS radar (ISR), or with other ISRs during PCA events. This observing technique allowed for ~24 h of almost continuous measurements of the meridional and zonal wind fields and thus permitted the measurements of atmospheric tides over this large altitude range. We determine amplitude and phase for both the diurnal and semi-diurnal tides showing the latter to be stronger as expected at these latitudes. We also present observations of a gravity wave during a quiet period indicating that PFISRs sensitivity is sufficiently high to obtain reliable spectral information even when electron densities are not enhanced by aurora or a PCA event and are as low as 10^9 e$^-$/m^3. These results show the capabilities of PFISR to study the neutral dynamics in the polar D-region and mesosphere and lower thermosphere (MLT) over an unprecedented altitude range.

1. Introduction

Studies of the D-region ionosphere and the neutral mesosphere and lower thermosphere (MLT) typically employ MF and HF radars measuring coherent backscatter from small-scale refractive index variations to determine neutral winds, tidal structures, gravity waves (GWs) and GW momentum fluxes, wave–wave interactions, and turbulence intensities, but necessarily at very coarse (~4 km) spatial resolution (e.g., Vincent, 1984; Fritts and Alexander, 2003). Similar studies at VHF allow for higher spatial resolution and precision, but also typically at restricted altitude intervals (e.g., Woodman and Guillen, 1974; Balsley and Carter, 1982; Hoppe and Fritts, 1995; Rastogi and Bowhill, 1976) UHF measurements are likewise restricted in altitude, except with very sensitive systems like the 430 MHz Arecibo Observatory (AO). Only recently, however, have measurement techniques at AO enabled the collection of IS data having high spatial and temporal resolution and high neutral wind accuracy (Zhou, 2000; Janches et al., 2006). At higher latitudes, wind estimates in the MLT have been obtained through IS measurements limited to periods during polar cap absorption (PCA) events or inferred from coherent returns from altitudes where polar mesosphere summer echoes (PMSE) represent strong radar backscatter enhancements (e.g., Hargreaves and Birch, 2005; La Hoz et al., 2006; Rapp et al., 2007; Nicolls et al., 2007, 2008). Measuring the D-region using IS is desirable because it is a direct measurement of the thermal fluctuations of the background plasma.

PMSE has been regularly observed at VHF in the polar summer D-region whereas UHF observations have been much less frequent. The altitude range, intensity, and fractional occurrence of PMSE are all strong functions of radar frequency, with the PMSE backscatter cross-section dropping by ~6 decades from 50 to 500 MHz (Rapp and Lubken, 2004). There have been only a few detections of PMSE at UHF, with the EISCAT 933 MHz radar (e.g., La Hoz et al., 2006), with the 1.29 GHz Sondrestrom IS radar (ISR)

* Corresponding author.
E-mail addresses: diego@cora.nwra.com (D. Janches), dave@cora.nwra.com (D.C. Fritts), michael.nicolls@sri.com (M.J. Nicolls), craig.heinselman@sri.com (C.J. Heinselman).

1364-6826/$ - see front matter © 2008 Elsevier Ltd. All rights reserved.
doi:10.1016/j.jastp.2008.08.015

(Cho et al., 1992), and the recent 26-beam measurement of PMSE morphology and aspect sensitivity using the new Poker Flat Incoherent Scatter Radar (PFISR) installed at the Poker Flat Research Range (65.13°N, 147.47°W) near Fairbanks, Alaska (Nicolls et al., 2007). Based on earlier data, Cho et al. (1996) noted that all UHF PMSE occurred during enhanced electron densities caused by particle precipitation. It appears to be unknown, however, how PMSE respond to variable auroral precipitation, or how the occurrence of PMSE is correlated with electron density variations at lower altitudes. Hence, measurements that specifically relate auroral precipitation, the occurrence of PMSE, and electron densities at PMSE and lower altitudes should be relevant to a variety of interests in the polar summer MLT. PFISR is ideally suited for studies of these processes. The focus in this paper is on measurements of D-region electron densities, PMSE occurrence, MLT neutral wind fields, and the insights into the dynamics provided.

2. Experiment description and data analysis

Our experiment with the 449.3 MHz 96-panel PFISR was intended to measure simultaneous radial velocities in four symmetric off-vertical beams that would allow for the determination of GW vector momentum fluxes using the Vincent and Reid (1983) technique. The primary motivation was the successful use of D-region IS at UHF for two-beam momentum flux measurements at AO (Zhou and Morton, 2006; Fritts et al., 2006; Fritts and Janches, 2008). The test presented in this work employed predefined beams with nominal directions north (zenith angle 10.5°, azimuth 1.81°), east (9.78°, 80.4°), south (11.44°, 179.69°), and west (9.27°, −82.82°). These beams were not exactly symmetric, but allowed us to compute mean horizontal winds and assess the technique.

Our measurements employed PFISR with a peak power of ~1.3 MW, a 13-baud barker code with 10 μs (1.5 km) bauds, 5 μs sampling, and a 2-ms IPP. The radar returns were sampled between 40 and 140 km range, and integration of 128 pulses in each of the beams enabled computation of spectra having full Doppler widths of 166 m s^{-1} and a frequency resolution of 3.9 Hz. Six successive spectra for each beam were averaged, yielding data with 6 s resolution. This experiment was performed for 24 h beginning 9 UT (local midnight) on 9 June 2007. We first focus on the first ~7 h of these observations when auroral activity was highest. There are, however, several other comparable intervals in the dataset from which similar conclusions could be drawn and as

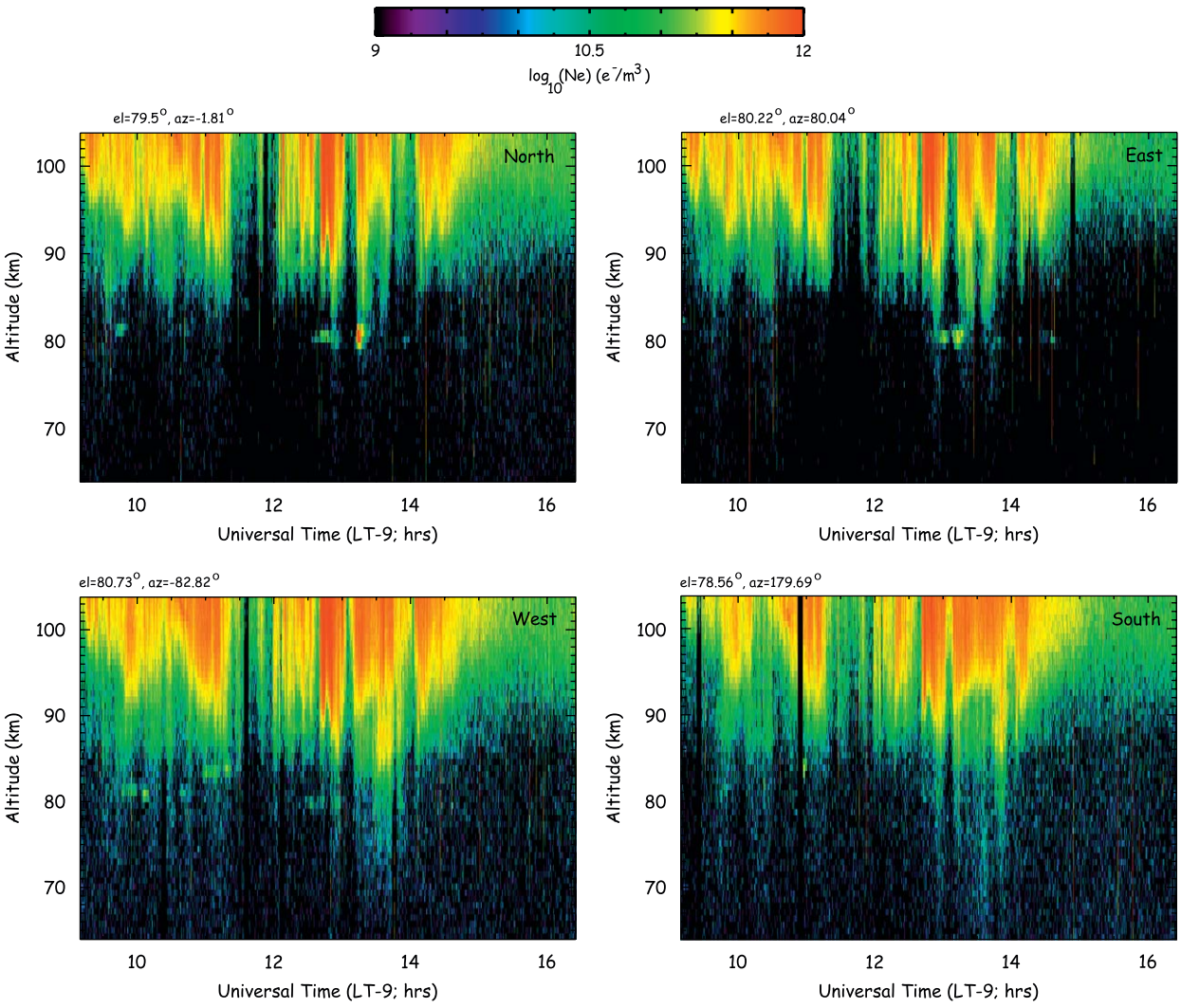

Fig. 1. N_e (except where PMSE enhances backscatter power) from ~9: 10 to 16:20 UT between 64 and 104 km in 6-s intervals in the four beams pointed north (upper left), east (upper right), west (lower left), and south (lower right).

it will be shown, even when the activity is not strong wind estimates can still be derived with enough resolution for tidal studies.

Doppler velocities in each beam and range gate were obtained from 16-min averages of individual 6-s spectra using a median filter.

3. Results and discussion

Estimates of measured electron densities (N_e) at altitudes from 64 to 104 km for each beam for the first ~7 h of the experiment are shown at 6 s resolution in Fig. 1 (~9–16 UT; LT = UT − 9). Errors of these estimates are on average 30%. The solar zenith angle varied during this period from ~91° to 68°, indicating that D-region ionization from the Sun was negligible in comparison to that from the aurora. In addition proton flux profiles derived from the GOES 11 satellite show very little activity from proton precipitation during the day of these observations with fluxes lower than 0.5 particles $cm^{-2}\,s^{-1}\,sr^{-1}$ for particles with energies greater than 10 MeV. The average K_p index for this day was 1.7 indicating a lack of significant influences by high energy particles. Thus the higher electron densities features presented in Fig. 1 are produced by normal auroral activity.

Referring to Fig. 1, we see modulations in N_e in all beams on time scales varying from a few minutes or less to several hours. Modulations at longer time scales, ~30 min and longer, appear to be largely coherent among the four beams and are apparently associated with spatial scales of auroral precipitation that are larger than the beam separations at MLT altitudes (~20–30 km at ~85 km altitude). Modulations at shorter time scales also exhibit correlations among all four beams on many occasions, but they are also often correlated among only a subset of the four beams, suggesting that they typically occur on smaller spatial scales. We also see that N_e enhancements decrease fairly uniformly with decreasing altitude, except for PMSE enhancements at ~79–85 km, and extend to altitudes below 70 km on multiple occasions. There were at least six PMSE events during our observation period. From these, we can observe that PMSE (1) always occur only accompanying N_e enhancements at higher altitudes, (2) are often embedded in the enhancements extending to lower altitudes, (3) are often absent at times of strong enhancements extending to very low altitudes, and (4) exhibit less coherence among the four beams than is seen in the N_e at other altitudes.

We also see in Fig. 1 that the north and east beam modulations, and the south and west beam modulations, appear more similar within pairs than between pairs, the N–E pair exhibits more variability at ~10 to 60-min periods from 12 to 14:30 UT, the S–W beam pair experiences deeper (larger) enhancements, and the N–E beam pair exhibits somewhat stronger PMSE, despite their lower N_e, at these times. Also, where PMSE backscatter power enhancements are clearly seen, primarily from 9:45 to 14:40 UT, there is a very strong agreement between the altitudes at which it is observed in all four beams, but again clear indications that the correlations are higher within the beam pairs above.

Fig. 2 compares PMSE reflectivity (black, left axis) with N_e at 77–78 and 100 km (blue and red, respectively, right axis) from 12 to 15 UT for which we observed the greatest N_e and PMSE reflectivity enhancements. For IS measurements, reflectivity is

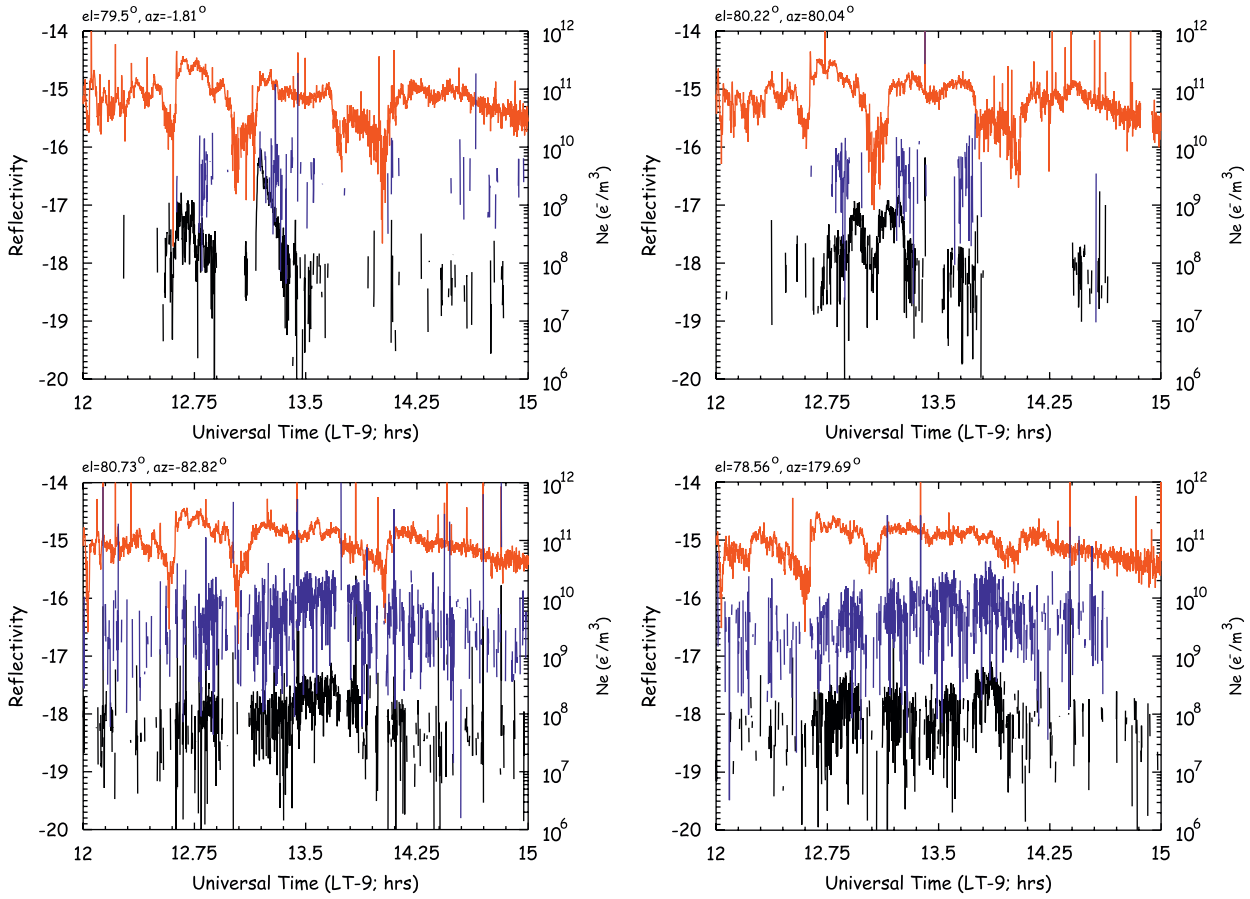

Fig. 2. PMSE reflectivity (black, left axis) and N_e averaged at ~77 km (blue, right axis) and at 100 km (red, right axis) from ~12 to 15 UT for each beam direction.

directly proportional to N_e (Evans, 1969). Several features of these plots are noteworthy. First, PMSE and backscatter power at 80 km, where PMSE is not observed, are highly correlated, and they are infrequently seen alone. There are a few intervals where PMSE is seen in isolation (upper left panel at 12.6 UT and upper right panel at 14.4 UT); there are also times when PMSE does not occur despite enhanced backscatter at 80 km (upper left panel at 14.75 UT). Thus PMSE may apparently occur with weaker auroral precipitation when PMSE conditions favor strong reflectivity (i.e. deep electron bite-outs and/or high Schmidt numbers). Conversely, PMSE can be suppressed even when N_e is enhanced at lower altitudes when PMSE reflectivity is weak. We also see that both PMSE reflectivity and N_e at 80 km are strongly correlated with enhanced N_e at 100 km, and very often exhibit maxima accompanying sharp increases in the 100-km backscatter power. This can be seen at a number of locations in Fig. 2, especially at 12.6 and 13.1 UT in all beams in which the 100 km enhancements are sudden.

Fig. 3 provides a very different perspective on the occurrence of D-region echoes, the correlations between PMSE and IS backscatter power, and the potential for applications to MLT dynamics. Shown are 16 min Doppler spectra spanning the central 60 m s^{-1} of the 166 m s^{-1} full-scale radial velocity spectra for each beam from ~12 to 14 UT. At the earlier times shown, there are only weak enhancements in IS backscatter power, and these typically occur together with weak (but higher power) PMSE. As noted in the discussion of Fig. 2, there are only a few occasions when one is seen without the other. At the intermediate times shown, all four beams exhibit significant enhancements in both IS backscatter power extending over all altitudes displayed and PMSE at their expected altitudes (~79 to 85 km). Especially when backscatter power is high, the spectral widths also clearly increase with altitude, as we expect for IS spectra at decreasing atmospheric densities. Interestingly, there are times at which PMSE are very strong and IS backscatter power is relatively weak, and vice versa. Indeed, there are 1, 2, and 3 and 15 min spectra in the east, west, and south beams at these times, respectively, during which PMSE cannot be detected, indicating that enhanced mean electron densities are not the only necessary condition for PMSE. The other condition relates to the scattering mechanism—likely the effects of an enhanced Schmidt number caused by the presence of charged ice, leading to either an

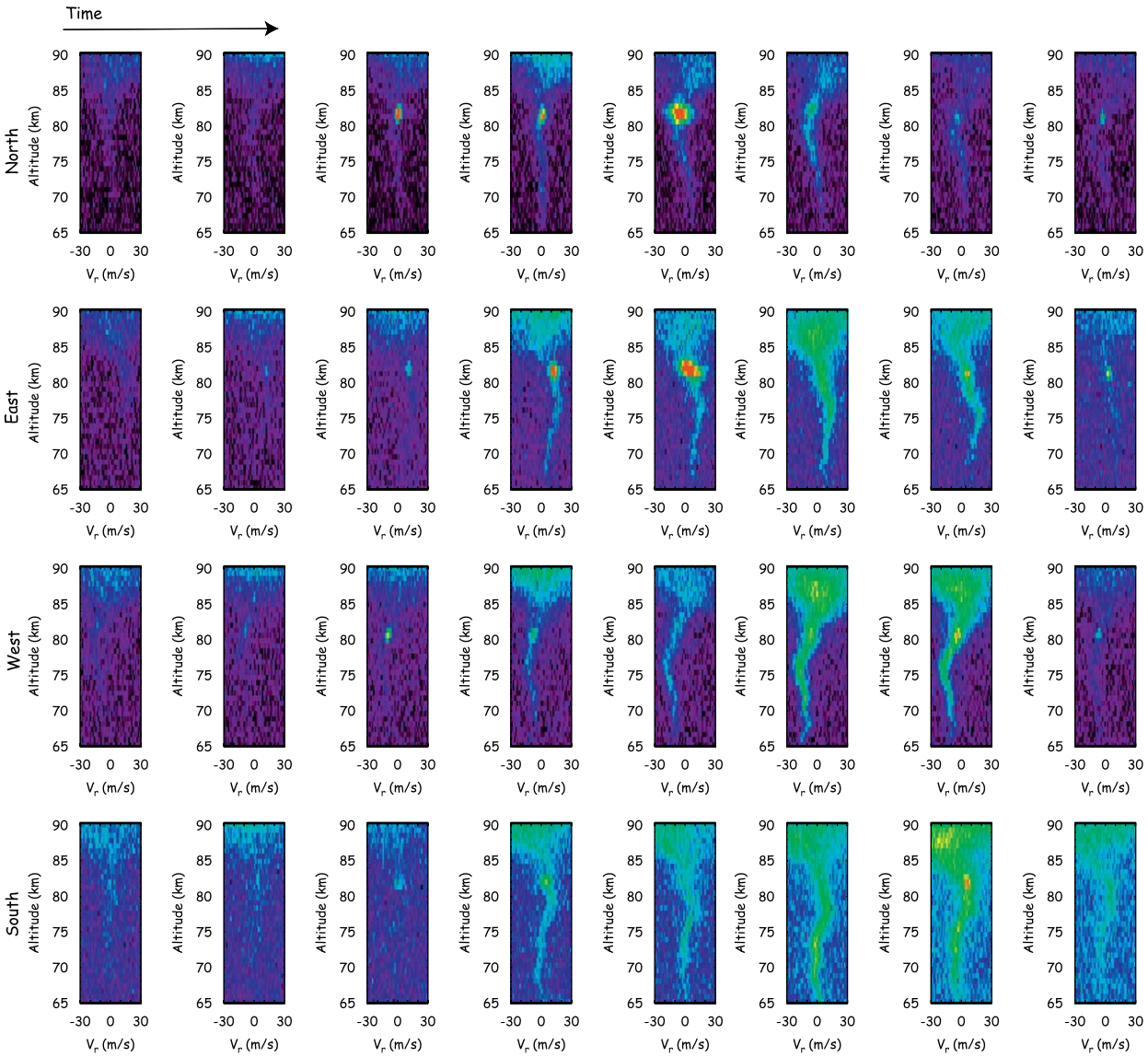

Fig. 3. Doppler spectra (16-min averages) for each beam from ~12 to 14 UT. Only weak IS backscatter power enhancements are seen at the earlier times, and these typically occur together with weak (but higher power) PMSE. At later times, IS power is much higher and spectra are better defined.

extension of the turbulent electron density fluctuation spectrum to the probing Bragg wavelength or to enhanced backscatter in other ways (e.g., Rapp and Lubken, 2004; La Hoz et al., 2006). In most cases, however, our observations indicate that PMSE may serve as a precursor for IS at lower altitudes in cases where N_e is increasing in time because of generally larger backscatter power and earlier backscatter signature. In general, scattering from the D-region becomes strong within minutes (~10 min) after PMSE is detected (Fig. 3). According to Rapp et al. (2002), PMSE precedes D-region IS scattering because its scattering cross section is much larger, causing it to be detected first for a radar of any sensitivity.

Doppler spectral means (and medians) also exhibit significant variations with altitude, suggesting N_e fluctuations are advected by radial velocities as high as ~20 m s^{-1}. N–S (and E–W) beams are seen to have largely anti-correlated velocities, suggesting primarily large-scale horizontal motions, and apparent vertical wavelengths range from a few to ~20 km. These radial velocities are very similar to those seen at these altitudes with the AO ISR (Zhou and Morton, 2006; Janches et al., 2006; Fritts and Janches, 2008). However, this is the first time velocities have been observed over such an extended range of altitudes in the polar summer MLT at UHF, except under PCA conditions. These observations suggest, therefore, the potential for extensive MLT dynamics contributions with the PFISR because of its enhanced sensitivity during enhanced auroral precipitation. To further quantify this capability, we show in Fig. 4 the 1 h mean zonal and meridional motions for 12:45–13:45 UT obtained by averaging the vector horizontal winds inferred for each beam pair. The errorbars on each profile indicate relatively high precision extending over altitudes from 64 to 89 km (horizontal wind uncertainties of ~3 m s^{-1} or less for most altitudes). Spectral widths increase with altitude (especially above 90 km) because of the decreasing collision frequency and increasing temperature until they are greater than our resolved spectra, at which point our measurement technique fails. The winds are also suggestive of the large-scale motions that we know from the previous studies to contribute to the large-scale wind fields at these altitudes. We expect, for example, a westward maximum at ~70−80 km and a southward maximum at ~85 km due to the influences of GWs on the zonal-mean circulation of the summer polar MLT (Fritts and Alexander, 2003). We expect to see significant modulations of the mean profiles with GW and tidal structures at vertical wavelengths from a few to ~20 km, and these are also seen in Fig. 4. Finally, the backscatter power profile in the right panel emphasizes the dominance of IS at the higher altitudes, the altitudes at which PMSE make the major contributions, and the weaker IS at lower altitudes to which radars with smaller PA products are not sensitive. The PMSE also exhibit large vertical excursions suggesting advection by high-frequency GWs that have been observed more continuously by VHF radars yielding higher S/N.

Fig. 5 shows hourly mean winds for the entire period of observation. The upper panels display the zonal and meridional winds derived from the raw data using a 15-min sliding window. These panels reveal downward phase motions spanning a range of periods, with the longer periods suggestive of diurnal and semi-diurnal tidal motions. Fits of 12- and 24-h periods to these data at each altitude are shown in the lower panels of Fig. 5. These results

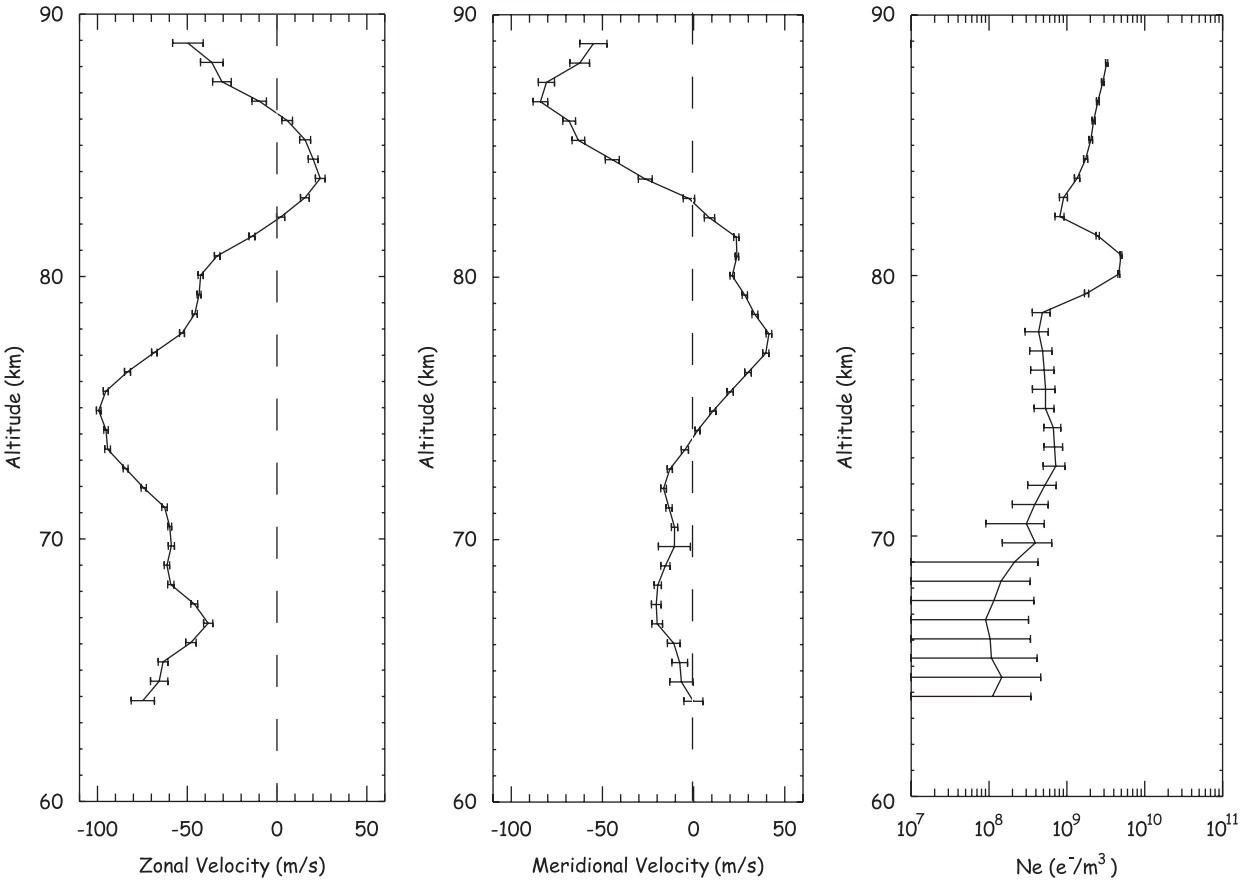

Fig. 4. Mean zonal and meridional motions (left and center panels) for the interval ~12:45−13:45 UT obtained by averaging the vector horizontal winds inferred for each beam pair. Errorbars indicate accuracy of a few m s^{-1} or better at most altitudes. The right panel shows electron density over the same interval.

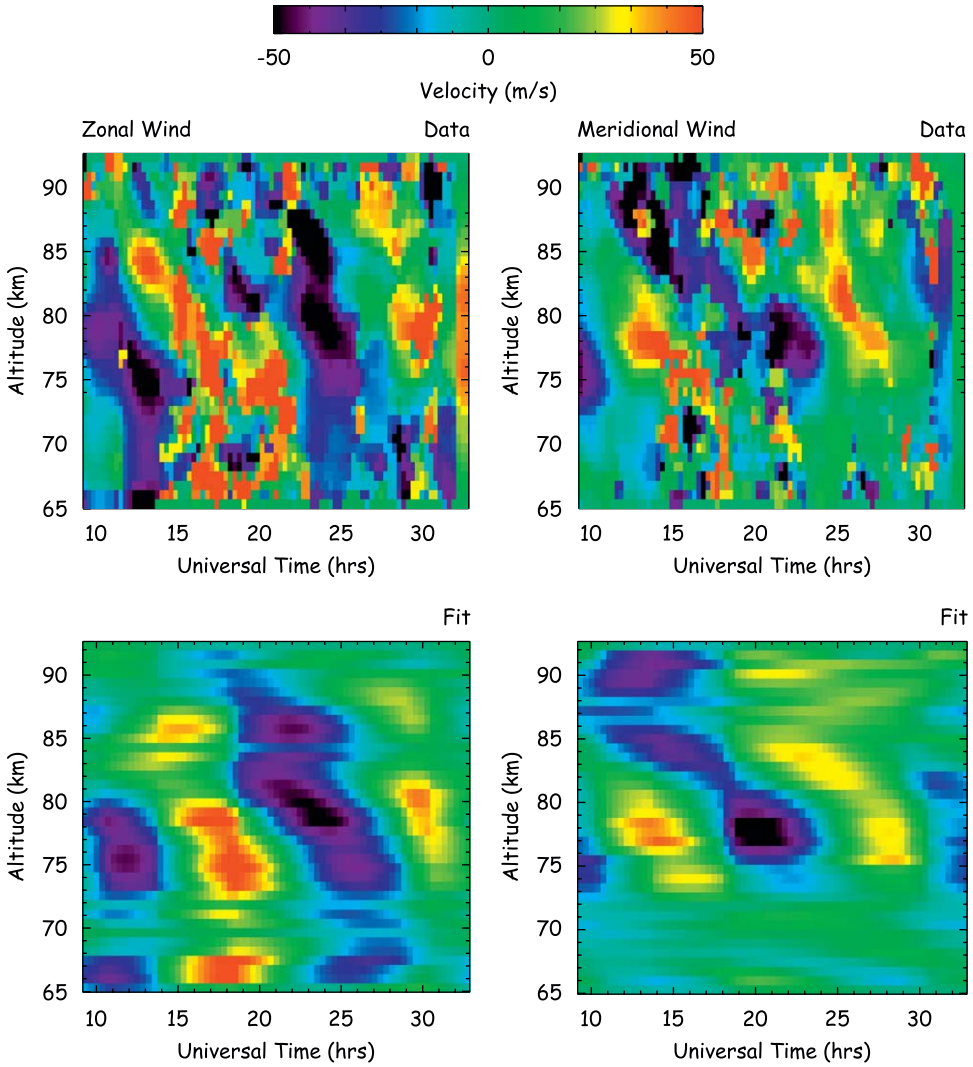

Fig. 5. Panels (a) and (b): zonal and meridional winds derived from the PFISR observations for a ~24 h period. Panels (c) and (d): modeled zonal and meridional winds derived from fitting a semi-diurnal and diurnal tidal components to the data presented in panels (a) and (b).

once again show the ability of PFISR to study neutral dynamics of the polar MLT with temporal resolution sufficient to define tidal and other low-frequency motions. Solid lines in Fig. 6 shows the amplitudes and phases of the 24- and 12-h fits to our data as displayed in Fig. 5. Also dashed lines are the tidal amplitudes predicted by the global scale wave model (GSWM) (Hagan and Forbes, 2002). The GSWM estimates represent monthly means which include the migrating and non-migrating diurnal and semi-diurnal components of the tide. It is evident, and perhaps not surprising, from this figure that fits to tidal periods for a single day may depart significantly from the monthly mean GSWM tidal climatology. What is not known is whether this is a result of a superposition of other low-frequency motions also present on this day, potential large tidal variability, or a failure of the GSWM to accurately describe the tides at this location.

There have been many previous studies addressing observed MLT tidal structures and their comparisons with theoretical and model predictions extending to high latitudes. The semi-diurnal tide typically achieves the largest responses at high latitudes. It also exhibits distinct seasonal behavior, significant differences between the two hemispheres, and evidence of migrating and non-migrating mode superpositions and interactions (see Manson et al., 2002; Riggin et al., 2003; Murphy et al., 2006, and references therein). Diurnal and terdiurnal tides also contribute to MLT structure, interactions and variability at high latitudes, but it is typically the semi-diurnal tide that achieves the largest amplitudes at those sites where such assessments have been performed. Semi-diurnal amplitudes are typically $10-20\,m\,s^{-1}$ at altitudes of 80–100 km (Singer et al., 2005), but have also been estimated to be as large as $50-90\,m\,s^{-1}$ for short intervals (Goldberg et al., 2006; Williams et al., 2006). Thus, there is clearly a history of large tidal amplitudes at high altitudes and latitudes, and further studies are required to define these dynamics more fully.

To further explore the ability of PFISR for neutral atmosphere dynamics studies, we utilize the same observing mode discussed above, but applied for MLT measurements that do not benefit from summer mesopause PMSE reflectivity enhancements and using a radar beam configuration employing seven, rather than four, beams. Our goal is to explore the sensitivity of D-region measurements to tidal and low-frequency GWs without significant ionization caused by either a PCA event or auroral activity. Examination of the N_e profiles during the late morning and afternoon of 15 September 2007, displayed in Fig. 7, indicates that auroral activity was negligible and that ionization in the D-region did not display the enhanced levels observed in Fig. 1. Here, N_e were estimated by integrating over the spectra (having Lorentzian shape) for the case of incoherent scatter radar from the D-region

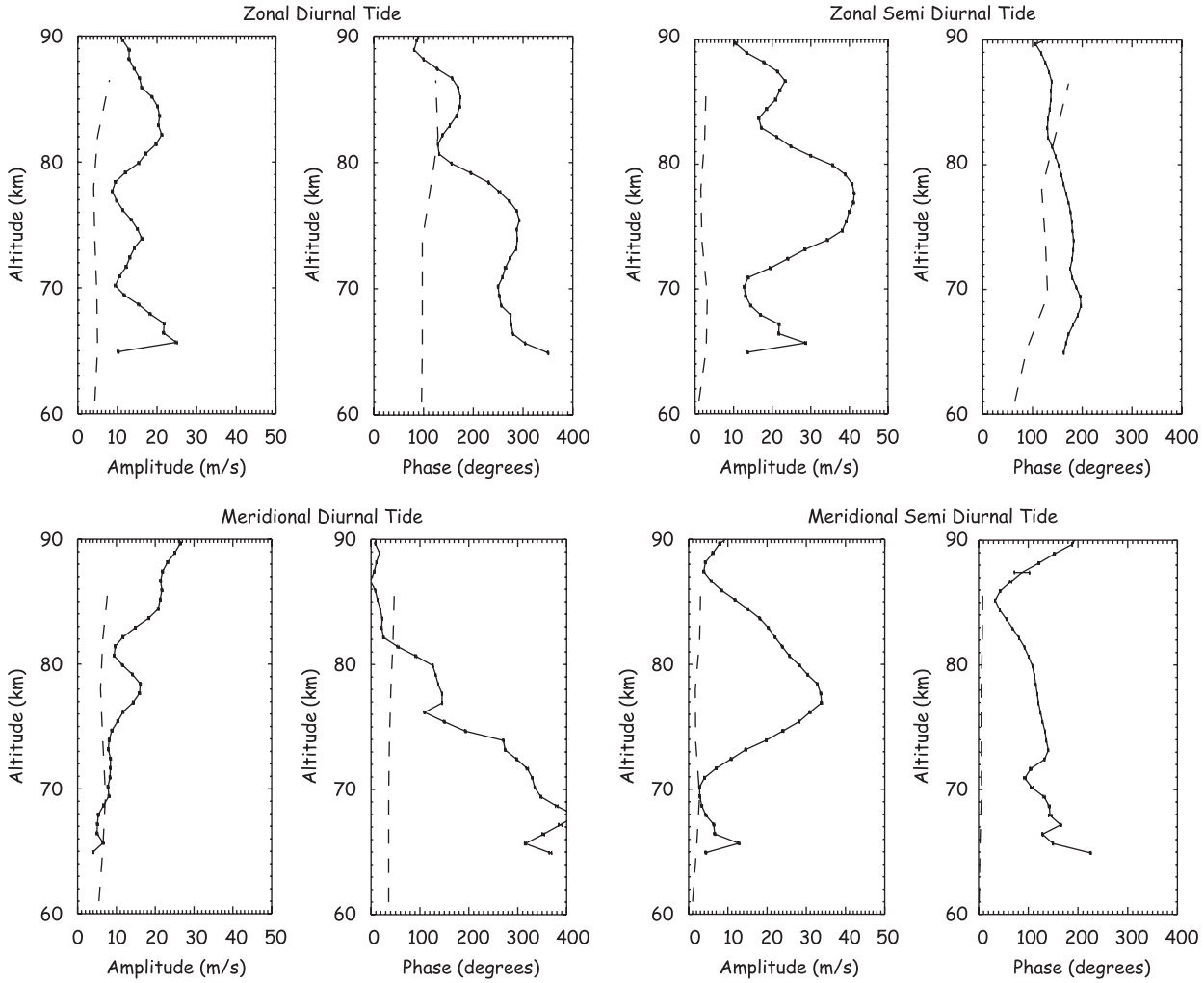

Fig. 6. Amplitude and phases of the semi-diurnal and diurnal tides resulted from the fits presented in Fig. 5(b) and (c). The dash lines in the amplitude panels are predictions using GSWM.

(Janches et al., 2006). This methodology reduces the errors (which are of the order of 10–20% for these data), because the noise bandwidth is effectively reduced, from the bandwidth of the samples (~100 kHz) to the bandwidth of the spectra (500 Hz). It appears from Fig. 7 that PFISR is sensitive to N_e values as low as $\sim 10^9\ e^-/m^3$. Fig. 8 shows hourly means of the zonal and meridional winds obtained during this measurements. Referring to Fig. 8, we also see evidence of an apparent low-frequency motion having downward phase progression, an apparent rotary wind structure with anti-cyclonic rotation with altitude (descending meridional wind maxima leading zonal maxima), and a relatively slow phase descent. Except for the first and last hours, during which N_e was lower and velocity estimates were less confident. These confirm the apparent quadrature phase relation between the zonal and meridional winds and suggest a dominant vertical wavelength of ~8−10 km and an apparent period of 10–12 h. Thus, PFISR is able to provide useful information on MLT dynamics even with relatively low D-region N_e densities.

4. Conclusions

We have described partial results of a four-beam experiment performed with the new PFISR at Poker Flat, Alaska on 9 June 2007 in the polar summer D-region and MLT. Our results reveal surprising sensitivity to D-region N_e and Doppler shifts of IS spectra extending down to ~64 km during times of significant auroral precipitation. Enhanced IS backscatter at lower altitudes was found to correlate with elevated backscatter power and inferred N_e at 100 km. We also noted a significant, but not complete, correlation of enhanced IS backscatter at these altitudes with PMSE at ~79−85 km. PMSE tended to precede enhanced N_e at lower altitudes as N_e is increasing, because of the higher backscatter power of PMSE in general at these altitudes and at the PFISR frequency. There were also occasions, however, during which IS backscatter was detected at lower altitudes, but PMSE were not observed. This indicates that enhanced auroral precipitation is a necessary, but not sufficient, condition for PMSE occurrence, because there are other dynamical and microphysical processes that also restrict PMSE occurrence on occasion.

The IS spectra obtained throughout the D-region during times of enhanced auroral precipitation also permitted sensitivity to MLT winds extending from ~64−89 km. These were found to yield measurements of zonal and meridional winds consistent with the previous measurements of mean winds and tidal and GW characteristics at these altitudes during polar summer. Given the importance of understanding these MLT dynamics, and the inability to measure them with this precision and resolution (except under PCA conditions) with radars at other locations, D-region measurements with PFISR under significant auroral precipitation conditions represent a valuable capability for more

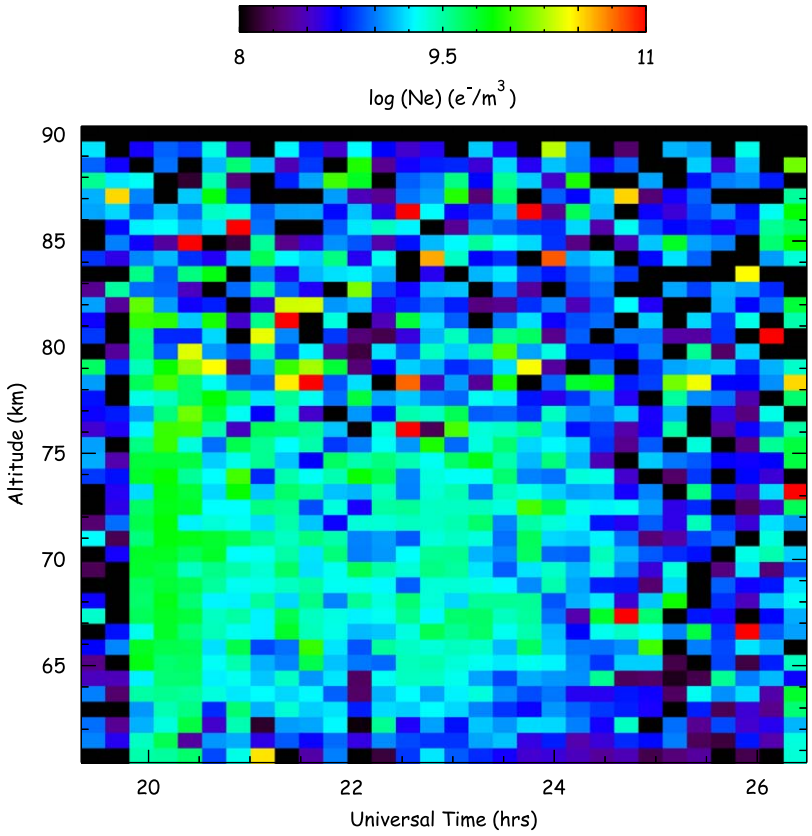

Fig. 7. Electron densities in the vertical direction measured on 15 September 15 2007. It is evident that these results are representative of a quiescent day.

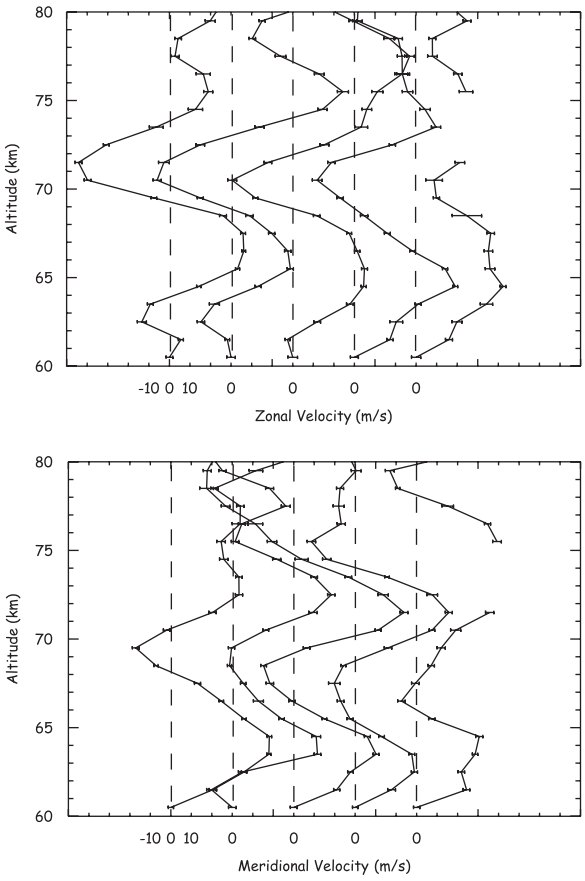

Fig. 8. Hourly mean zonal and meridional winds.

comprehensive MLT studies in the future. Our results show the presence of both diurnal and semi-diurnal tides with the latter having a larger response in our data. We hope to employ this technique on multi-day measurements that would contribute to our knowledge of tidal variability in the future.

We have also presented observations of N_e and a GW showing that PFISR D-region measurements can be extended to periods without aurora or PCA electron density enhancements. Surprisingly, reliable spectral information can be obtained when N_e is as low as $10^9\,e^-/m^3$. These results show the capabilities of PFIR to study the neutral dynamics in the polar D-region and MLT in an unprecedented altitude range.

Acknowledgments

The PFISR is operated by SRI International under a cooperative agreement with the National Science Foundation. This research was supported under NSF Grants ATM-05311464, ATM-0525655, ATM-0436703 and OPP-0438777 and by AFOSR contract FA9550-06-C-0129. The authors wish to thank M. Rapp for useful discussions.

References

Balsley, B.B., Carter, D.A., 1982. The spectrum of atmospheric velocity fluctuations at 8 and 86 km. Geophysics Research Letters, 465–468.

Cho, J.Y.N., Kelley, M.C., Heinselman, C.J., 1992. Enhancement of Thomson scatter by charged aerosols in the polar mesosphere: measurements with a 1.29 GHz radar. Geophysics Research Letters 19, 1097–1100.

Cho, J.Y.N., Alcala, C.M., Kelley, M.C., Swartz, W., 1996. Further effect of charged aerosols on summer mesospheric radar scatter. Journal of Atmospheric and Solar-Terrestrial Physics 58 (6), 661–672.

Evans, J., 1969. Theory and practice of ionosphere study by Thomson scatter radar. Proceedings of the IEEE 57 (4), 496–530.

Fritts, D.C., Alexander, M.J., 2003. Gravity dynamics and effects in the middle atmosphere. Reviews of Geophysics 41, 3-1–3-64, doi:10.1029/2001RG000106.

Fritts, D.C., Janches, D., 2008. Dual-beam measurements of gravity waves over Arecibo: reevaluation of wave structure, dynamics, and momentum fluxes. Journal of Geophysical Research 113, 1–13, D05112, doi:10.1029/2007JD008896.

Fritts, D.C., Janches, D., Riggin, D.M., Stockwell, R., Sulzer, M.P., Gonzalez, S., 2006. Gravity waves and momentum fluxes in the MLT using 430 MHz dual-beam measurements at Arecibo: 2. Frequency spectra, momentum fluxes, and variability. Journal of Geophysics Research 111.

Goldberg, R.A., Fritts, D.C., Schmidlin, F.-J., Williams, B.P., Croskey, C.L., Mitchell, J.D., Friederich, M., Russell III, J.M., Blum, U., 2006. The MaCWAVE program to study gravity wave influences on the polar mesosphere. Annales de Geophysique 1159–1173.

Hagan, M.E., Forbes, J.M., 2002. Migrating and nonmigrating diurnal tides in the middle and upper atmosphere excited by tropospheric latent heat release. Journal of Geophysical Research 107 (D24), 4754–4762, doi:10.1029/2001JD001236.

Hargreaves, J.K., Birch, M.J., 2005. On the relations between proton influx and D-region electron densities during the polar-cap absorption event of 28–29 October 2003. Annales de Geophysique 23, 3267–3276.

Hoppe, U.-P., Fritts, D., 1995. High resolution measurements of vertical velocity with the EISCAT VHF radar, 1,1 motion fields characteristics and measurements biases. Journal of Geophysics Research 100, 16,813–16, 826.

Janches, D., Fritts, D.C., Riggin, D.M., Sulzer, M.P., Gonzalez, S., 2006. Gravity waves and momentum fluxes in the MLT using 430 MHz dual-beam measurements at Arecibo: 1. measurements, methods, and gravity waves. Journal of Geophysical Research (Atmospheres) 111, D18107, doi:10.1029/2005JD006882.

La Hoz, C., Havnes, O., Naesheim, L.I., Hysell, D.L., 2006. Observations and theories of polar mesospheric summer echoes at a Bragg wavelength of 16 cm. Journal of Geophysics Research 111.

Manson, A.H., Meek, C., Hagan, M., Koshyk, J., Franke, S., Fritts, D., Hall, C., Hocking, W., Igarashi, K., MacDougall, J., Riggin, D., Vincent, R., 2002. Seasonal variations of the semi-diurnal and diurnal tides in the MLT: multi-year MF radar observations from 2 to 70 deg N, modelled tides (GSWM, CMAM). Annales de Geophysique 20, 661–677.

Murphy, D.J., Forbes, J.M., Walterscheid, R.L., Hagan, M.E., Avery, S.K., Aso, T., Fraser, G.J., Jarvis, M.J., Riggin, D.M., Fritts, D.C., Tsutsumi, M., Vincent, R.A., 2006. A climatology of tides in the Antacrtic mesosphere. Journal of Geophysical Research 111, D23104, doi:10.1029/2005JD006803.

Nicolls, M.J., Heinselman, C.J., Hope, E.A., Ranjan, S., Kelley, M.C., Kelly, J.D., 2007. Imaging of polar mesosphere summer echoes with the 450 MHz poker flat advanced modular incoherent scatter radar. Geophysical Research Letters 34, L20102, doi:10.1029/2007GL031476.

Nicolls, M.J., Kelley, M.C., Varney, R.H., Heinselman, C.J., 2008. Spectral observations of polar mesospheric summer echoes at 33 cm (450 MHz) with the Poker Flat Incoherent Scatter Radar. Journal of Atmospheric and Solar-Terrestrial Physics, this issue, doi:10.1016/j.jastp.2008.04.019.

Rapp, M., Lubken, F.-J., 2004. Polar mesosphere summer echoes (PMSE): review of observations and current understanding. Atmospheric Chemistry and Physics 4, 2601–2633.

Rapp, M., Gumbel, J., Lubken, F.-J., Latteck, R., 2002. D region electron number density limits for the existence of polar mesosphere summer echoes. Journal of Geophysics Research 107 (D14).

Rapp, M., Strenlnikova, I., Gumbel, J., 2007. Meteoric smoke particles: evidence from rocket and radar techniques. Advances in Space Research 40, 809–817.

Rastogi, P.K., Bowhill, S.A., 1976. Gravity waves in the equatorial mesosphere. Journal of Atmospheric and Solar-Terrestrial Physics 38, 50–61.

Riggin, D.M., Meyer, C.K., Fritts, D.C., Jarvis, M.J., Murayama, Y., Singer, W., Vincent, R.A., Murphy, D.J., 2003. MF radar observations of seasonal variability of semidiurnal motions in the mesosphere at high northern and southern latitudes. Journal of Atmospheric and Solar-Terrestrial Physics 65, 483–493.

Singer, W., Latteck, R., Hoffman, P., Williams, B.P., Fritts, D.C., Murayama, Y., Sakanoi, K., 2005. Tidal and planetary waves during the MaCWAVE/MIDAS summer rocket program. Geophysical Research Letters MaCWAVE special issue, 32, L07S90, doi:10.1029/2004GL021606.

Vincent, R.A., 1984. MF/HF radar measurements of the dynamics of the mesopause region—a review. Journal of Atmospheric and Solar-Terrestrial Physics 46, 961–974.

Vincent, R.A., Reid, I.M., 1983. HF Doppler measurements of mesospheric momentum fluxes. Journal of Atmospheric Sciences 40, 1321–1333.

Williams, B.P., Fritts, D.C., She, C.Y., Baumgarten, G., Goldberg, R.A., 2006. Gravity wave propagation tidal interaction and instabilities in the mesosphere and lower thermosphere during the winter 2003 MaCWAVE rocket campaign. Annales de Geophysique 24, 1199–1208.

Woodman, R.F., Guillen, A., 1974. Radar observations of winds and turbulence in the stratosphere and mesosphere. Journal of Atmospheric Sciences 31, 493–505.

Zhou, Q., Morton, Y.T., 2006. A case study of mesospheric gravity wave momentum flux and dynamical instability using the Arecibo dual beam incoherent scatter radar. Geophysics Research Letters 33.

Zhou, Q.H., 2000. Incoherent scatter radar measurement of vertical winds in the mesosphere. Geophysics Research Letters 27 (12), 1803–1806.